International Journal of Advanced Research in Chemical Science (IJARCS)
Volume 2, Issue 12, December 2015, PP 15-24
ISSN 2349-039X (Print) & ISSN 2349-0403 (Online)
www.arcjournals.org

In Situ Studies of $LaMnO_3$ Phases Formation When used of Different Precursors

Anzhela G. Rudskaya, Natal'aya B. Kofanova, Michael F. Kupriyanov

Southern Federal University, Department of Physics, Rostov-on-Don
Zorge street, 5, Russia
arudskaya@yandex.ru, nbkofanova@sfedu.ru, kupriyanovmf@sfedu.ru

Abstract: *$LaMnO_3$ specimens were synthesized with using of different precursors on X-ray diffractometer (method in situ). It was established that the cubic nano- and microcrystalline perovskite phases starts to form in the temperature range 400 – 600 °C. Synthesized $LaMnO_3$ specimens at room temperature have stoichiometric and nonstoichiometric perovskite-type phases of different symmetry: Pnma (solid state synthesis) and $R\bar{3}c$ (wet methods of precursors' preparation – sorption, co-precipitation and sol-gel)*

Keywords: *$LaMnO_3$, perovskite, micro- and nanostructures, solid state synthesis, sorption, co-precipitation, sol-gel*

Abbreviations:

CMR: Colossal magnetoresistance

PM: Paramagnetic

FM: Ferromagnetic

SSS: Solid state synthesis

PXRD: Powder X-ray diffraction

FWHM: Full width half maximum

CSR: Coherent scattering region

1. INTRODUCTION

During the last decade there have been carried extensive searches and investigations of various oxide systems, which can be used as multifunctional materials, possessing combination of electric, dielectric, ferroelectric, ferroelastic, magnetic and other properties. Such materials can be used in different kinds of micro- and nanostructured materials of the new generation such as thin films, superlattices, nanofibers, nanotubes and nanowires [1-10]. It was established that in $LaMnO_3$ thin films at room temperature appear colossal magnetoresistance and different types of charge and orbital ordering [11].

It is previously established that in the solid solutions on basis of $LaMnO_3$ there can be seen phase transitions of the type paramagnetic semiconductor – ferromagnetic metal (PM – FM transition) [12, 13] and the effects of the colossal magnetoresistance (CMR) [14, 15].

In [16] reviewed various models of solid solutions based on $LaMnO_3$. In these models, it is assumed that in the magnetoresistive effect the main role is played by the electron-phonon interactions, which compete with the effects of the double exchange. These models, was explained the relationship between changes of the properties of solid solutions (from the insulator to the metal) with increasing content of additional components to $LaMnO_3$ with structure changes. It is important that superexchange interaction *B*-type ions (Mn or other *d*-elements) determines the magnitude of the CMR effects at temperature phase transitions. Therefore, the studies of solid solutions based on $LaMnO_3$ are of considerable interest.

Among such solid solutions are known solid solutions with La ions substitutions on mono-, di- and trivalent ions (for example, Ag, K, Na; Ca, Sr, Ba, Pb; Bi and *R* – Y, Ce, Pr, Sm) and Mn ions on *B* ions (for example, *B* – V, Cr, Fe, Co, Ni, Cu) [17-21].

It is stated that physical properties of the $LaMnO_3$ and its solid solutions widely vary depending on the conditions of samples preparation [22-25]. It's clear that various ways of such materials preparation cause structural defects of different kinds.

Solid state synthesis peculiarities of stoichiometric and nonstoichiometric $LaMnO_3$ are particularly described in [13, 26, 27]. In [23, 28, 29] samples are made with the help of the mechanochemical activation method. In [30, 31] in the process of $LaMnO_3$ synthesis there was used the method of chemical co-precipitation. Sol-gel method is used for $LaMnO_3$ preparation with the particles of different sizes [32]. $LaMnO_3$ synthesis made by hydrothermal method is described in [33]. $LaMnO_3$ synthesis is possible with the help of microwave plasma [34]. Nonstoichiometric samples of $LaMnO_{3+\delta}$ are produced by the spray drying and glycine-nitrate methods [24, 35]. In [36, 37] the citrate pattern of synthesis (Pechini method) is used for nonstoichiometric samples preparation. The results of $LaMnO_3$ synthesis by Pechini method are described in [25, 32, 38, 39].

Present article describes the results of studying of $LaMnO_3$ structure formation from nano- to micro structured states. In this paper we studied $LaMnO_3$ formation by solid state synthesis (SSS) method and wet synthesis methods (sorption, co-precipitation, sol-gel). In SSS metod of the main mechanism of the synthesis is the diffusion of atoms forming the final product. At the same time, there remain problems of homogeneity of the final product. When using wet methods homogeneity achieved a good mix of organometallic complexes in the liquid phase. In this preparation of the pure product may be a problem. These problems are solved by optimizing the temperature and time of precursors annealing.

In present work $LaMnO_3$ specimens were synthesized with using of different precursors on *X*-ray diffractometer (*in situ* method).

2. MATERIALS AND METHODS

Stoichiometric mixture $La(OH)_3$ and MnO_2 was used as a precursor for $LaMnO_3$ synthesis in the solid state synthesis method. Next precursors are made by the wet methods for $LaMnO_3$ synthesis.

The formation of the precursor ($La[Mn(OH)_3(NO_3)_3]$ in the method of sorption is carried out from an aqueous solution of $Mn(NO_3)_2$, to which is added an aqueous solution of 10% NH_4OH for preparing $Mn(OH)_2$. Then $Mn(OH)_2$ is oxidized aqueous solution of 10% H_2O_2 to $Mn(OH)_3$, which is mixed in stoichiometric proportion with an aqueous solution of $La(NO_3)_3$. The resulting solution is kept for 24 hours at room temperature and dried.

In the coprecipitation method, a precursor for synthesis $LaMnO_3$ was prepared from a stoichiometric mixture of aqueous solutions of $Mn(NO_3)_2$ and $La(NO_3)_3$ with 10% NH_4OH held by the scheme:

a. $Mn(NO_3)_2 + 2NH_4OH \rightarrow Mn(OH)_2\downarrow + 2NH_4NO_3$.

b. $2Mn(OH)_2 + H_2O_2 \rightarrow 2MnO(OH)\downarrow + 2H_2O$.

c. $La(NO_3)_3 + 3NH_4OH \rightarrow La(OH)_3\downarrow + 3NH_4NO_3$.

The resulting mixture solution $La(OH)_3$ and $MnO(OH)$ annealed at $T = 120$ °C resulting in a homogeneous mixture was formed nanostructures Mn_2O_3 and La_2O_3.

Synthesis $LaMnO_3$ with using a sol-gel method is carried out from an aqueous solutions of $La(NO_3)_3$ and $Mn(NO_3)_2$ with the addition of glycerin as the organic matrix. When heated, the mixture is polymerized to form a gel with homogeneous nanoscale.

Prepared precursors were put into the thermal chamber on the X-ray upgraded diffractometer DRON-3M and were heated up from the room temperature to high temperatures (700 – 1180 °C) with registration of diffraction profiles at different temperatures T_i. The heating rate of the samples was following: the heating (20 K/min) to T_1 → stable temperature (10 min) → powder X-ray diffraction (PXRD) (15 min) → the heating to the next constant temperature T_2 and so on up to the maximum heating temperature. After the sample cooling to the room temperature there was conducted PXRD of the produced $LaMnO_3$ and SEM observations on FE-SEM Zeiss SUPRA 25.

PXRD was conducted on CuK_α – radiation (Ni filter) with the using of Bregg-Brentano (θ-2θ) method in the interval $20 \le 2\theta \le 75$ degree by step-wise sample-detector angular scanning (step (2θ) = 0.02 degree, τ = 1 s). Diffraction profiles were processed with the help of computer program PowderCell 2.4 and 2.3 [40]. Definition accuracy of unit cells linear parameters was

±0.001 Å, and it was 0.05 degree for angular parameters. Profile factors of invalidation (R_p) were used as structural parameters refinement criteria. R_p – factors are determined for the samples counting those containing not only $LaMnO_3$ but also La_2O_3, Mn_2O_3 and other phases in small quantities (up to 5-10 %).

3. RESULTS AND DISCUSSION

3.1. Effects of $LaMnO_3$ Solid-Phase Synthesis Reactions

In the figure 1 there are presented fragments of diffraction profiles, produced during $LaMnO_3$ synthesis with the using of solid state reactions at different temperatures of annealing (T_{ann}). It has been stated that $La(OH)_3$ transformation into La_2O_3–I (hexagonal, a_H = 4.06, c_H = 6.41 Å) finishes till 400 °C. Following further heating at 700–750 °C temperatures La_2O_3–I isostructurally turns into La_2O_3–II (hexagonal, a_H = 3.94, c_H = 6.13 Å) with structure compression. Such changes of structures are typical for transitions from nanocrystalline to microcrystalline states. Structural changes of MnO_2 play an important role in $LaMnO_3$ synthesis kinetics. MnO_2 is used as an initial component. It is known, that various manganese oxides (MnO, Mn_2O_3, Mn_3O_4, MnO_2) turn into each other at differing temperatures (for example, MnO_2 converts into Mn_2O_3 at T_{ann} about 535 °C).

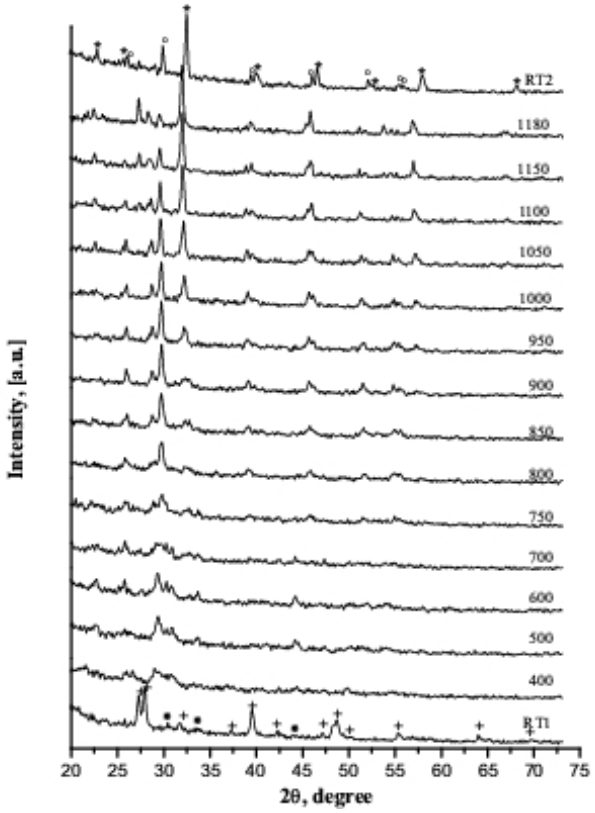

Figure1. *Diffraction profiles during $LaMnO_3$ synthesis by solid state reactions method ($400 \le T_i \le 1180$ °C). In the figure there are marked by the symbols: + – $La(OH)_3$; ● – MnO_2; * – $LaMnO_3$; o – La_2O_3; RT1 – diffraction profile of the initial precursors at room temperature; RT2 – diffraction profile of the sample after cooling to room temperature.*

Temperatures start of solid-phase synthesis T_{sr} can be determined by thermodynamic parameters ΔH and S (ΔH – changes of enthalpies, S – entropies) for La_2O_3, Mn_2O_3 and $LaMnO_3$ with relations

$$\Delta H° = 2\Delta H°(LaMnO_3) - [\Delta H°(La_2O_3) + \Delta H°(Mn_2O_3)],$$

$$\Delta S° = 2S°(LaMnO_3) - [S°(La_2O_3) + S°(Mn_2O_3)].$$

According to [41–43] for $LaMnO_3$: $\Delta H°$= -1438 kJmol^{-1}, $S°$=116.7 Jmol^{-1}K^{-1}; for La_2O_3: $\Delta H°$= -1793 kJmol^{-1}, $S°$=128.1 Jmol^{-1}K^{-1}; for Mn_2O_3: $\Delta H°$= -958 kJmol^{-1}, $S°$=110.5 Jmol^{-1}K^{-1}. A simple estimate $T_{sr} = \Delta H°/\Delta S°$ leads to a value T_{sr} ~ 1030 K.

In the table 1 shown structural parameters of $LaMnO_3$ perovskite cubic unit cells at different temperatures. Following minimum T_{ann} (400 °C) there appears cubic perovskite phase (P_0) with

abnormally large parameter of the unit cell (a_c = 4.09 Å). Diffraction reflections of the phase P_0 at 400 °C is characterized by large full width half maximum (FWHM) (up to 1 degree), which can be evidence of significant crystallite structure imperfection and also minimally of coherent scattering region (CSR). The average CSR (<*D*>) size of phase P_0 at 400 °C equals 100–200 Å. In the range of 400 to 700 °C there occurs decreasing FWHM of phase P_0 diffraction reflections, which can be evidence of the CSR growth of this phase up to about 500–600 Å. At 700 < T_{ann} < 750 °C P_0 phase completely transforms into phases P_1 and/or P_2.

Table1. *Structural parameters of $LaMnO_3$ perovskite cubic unit cells at different temperature of annealing during solid state synthesis*

T_{ann}, °C	Perovskite sub-cell parameters, Å			R_p
	a_0	a_1	a_2	
RT1	$La(OH)_3$ + MnO_2			0.041
400	4.085(1)*	–	–	0.078
500	4.092(1)	–	–	0.075
600	4.095(1)	3.855(1)	3.762(1)	0.070
700	4.094(1)	3.866(1)	3.759(1)	0.069
750	–	3.868(1)	3.758(1)	0.045
800	–	3.900(1)	3.811(1)	0.043
850	–	3.913(1)	3.864(1)	0.039
900	–	3.915(1)	3.871(1)	0.038
950	–	3.930(1)	3.907(1)	0.035
1000	–	3.929(1)	–	0.033
1050	–	3.940(1)	–	0.031
1100	–	3.946(1)	–	0.031
1150	–	3.953(1)	–	0.032
1180	–	3.954(1)	–	0.033

**) effective average cell parameters*

Phase transformation of MnO_2 to Mn_2O_3 at 530–540 °C preserves an octahedral coordination of Mn-ions with oxygen atoms. In our experiment this conversion is apparently not complete. In the range of temperatures from 500 to 600 °C there start to form perovskite phases P_1 ($LaMn^{3+}O_3$), and P_2 ($La_{2/3}Mn^{4+}O_3$). Cubic unit cells parameters of phases P_1 and P_2 (a_1 = 3.855 Å, a_2 = 3.762 Å, at T_{ann} = 600 °C). It is known that lengths of bonds $l(Mn^{4+}–O^{2-})$ in MnO_2 approximately 1.88 Å, and $l(Mn^{3+}–O^{2-})$ in Mn_2O_3 amounts to 2.00 Å. These differences reflect in a_1 and a_2 parameters. Unit cell parameters of phase P_1 (a_1) changes quite monotonously with the T_{ann} increase, meaning ordinary, almost linear thermal expansion, while parameter a_2 of phase P_2 abruptly increases in the interval of 750 < T_{ann} < 850 °C. We consider this fact as the result of increased La occupation in the perovskite structure P_2, with Mn^{4+} into Mn^{3+} transition. At the same time on the X-ray diffraction profiles there may be observed noticeable decrease of La_2O_3-II diffraction reflections intensities, giving evidence that it's connected in perovskite P_2 structure. At temperatures 950 < T_{ann} < 1000 °C phase P_1 finally forms from phase P_2. Monophase $LaMn^{3+}O_3$ maintains when the sample is cooled to room temperature. PXRD analyses of the synthesized $LaMnO_3$ allowed to state that at room temperature symmetry is orthorhombic with space group *Pnma* and unit cell parameters: a_O = 5.479(5), b_O = 7.763(5), c_O = 5.523(5) Å. The refined structural and positional atomic parameters are well coordinated with literary data.

3.2. Wet Methods of Synthesis: Sorption (I), Co-Precipitation (II), Sol-Gel (III)

In the figures 2 – 4 there are presented diffraction profiles at different temperatures of $LaMnO_3$ precursors annealing, produced by the methods I – III. The processes of phase formation of perovskite phase $LaMnO_3$ from precursors, produced by the methods I and II start (as well as in solid state synthesis) from the formation of two phases (P_1 and P_2). One P_1 phase forms by using method III. Formation of $LaMnO_3$ perovskite phases proceeds in various temperature intervals for different methods of precursors preparation: methods I and III – 550 < T_{ann} < 600 °C; method II – 500 < T_{ann} < 800 °C; solid state synthesis – 400 < T_{ann} < 1000 °C. In the table 2 there are presented structural parameters of perovskite cubic unit cells of $LaMnO_3$ at different T_{ann}, produced by the methods I – III.

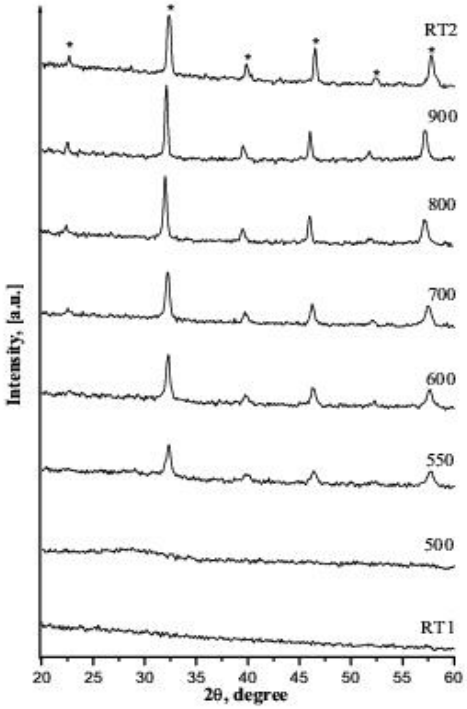

Figure2. *Diffraction profiles at different temperature of annealing ($500 \leq T_{ann} \leq 900$ °C) of $LaMnO_3$ precursors, produced by the sorption method. In the figure there are marked by the symbols: * – $LaMnO_3$; RT1 – diffraction profile of the initial precursors at room temperature; RT2 – diffraction profile of the sample after cooling to room temperature.*

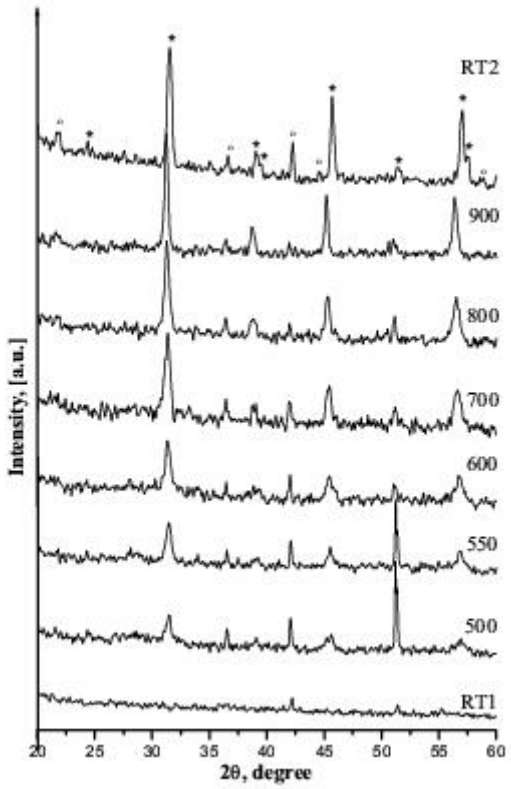

Figure3. *Diffraction profiles at different temperature of annealing ($500 \leq T_{ann} \leq 900$ °C) of $LaMnO_3$ precursors, produced by the co-precipitation method. In the figure there are marked by the symbols: * – $LaMnO_3$; o – MnO_2; RT1 – diffraction profile of the initial precursors at room temperature; RT2 – diffraction profile of the sample after cooling to room temperature.*

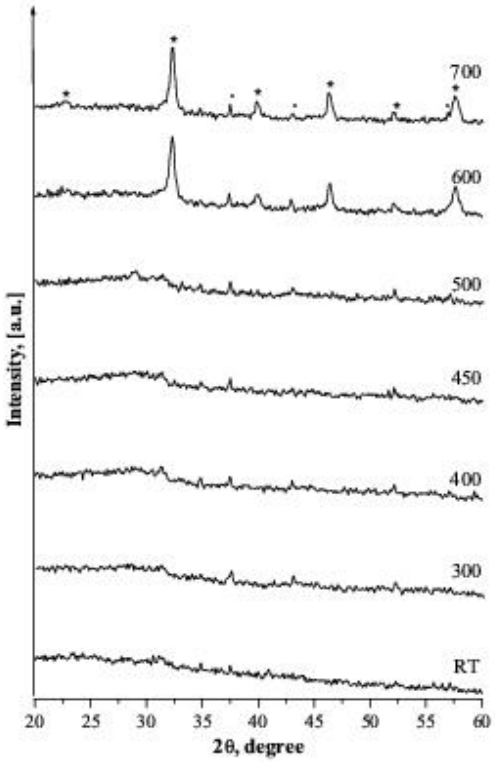

Figure4. *Diffraction profiles at different temperature of annealing ($300 \leq T_{ann} \leq 700$ °C) $LaMnO_3$ precursors, produced from sol-gel mixtures. In the figure there are marked by the symbols: * – $LaMnO_3$; o – MnO_2; RT – diffraction profile of the initial precursors at room temperature*

Table2. *Structural parameters of $LaMnO_3$ perovskite cubic unit cells at different temperature of annealing, produced by the methods I – III*

T_{ann}, °C	Method I			Method II			Method III	
	a_1, Å	a_2, Å	R_p	a_1, Å	a_2, Å	R_p	a_1, Å	R_p
500	–	–	–	4.016(5)	3.980(5)	0.055	–	–
550	3.933(5)	3.906(5)	0.031	4.005(5)	3.972(5)	0.050	–	–
600	3.929(5)	3.914(5)	0.032	4.009(5)	3.970(5)	0.049	3.913(5)	0.031
700	3.922(5)	–	0.028	3.996(5)	3.966(5)	0.047	3.918(5)	0.029
800	3.935(5)	–	0.028	3.926(5)	–	0.044	–	–
900	3.947(5)	–	0.027	3.936(5)	–	0.041	–	–

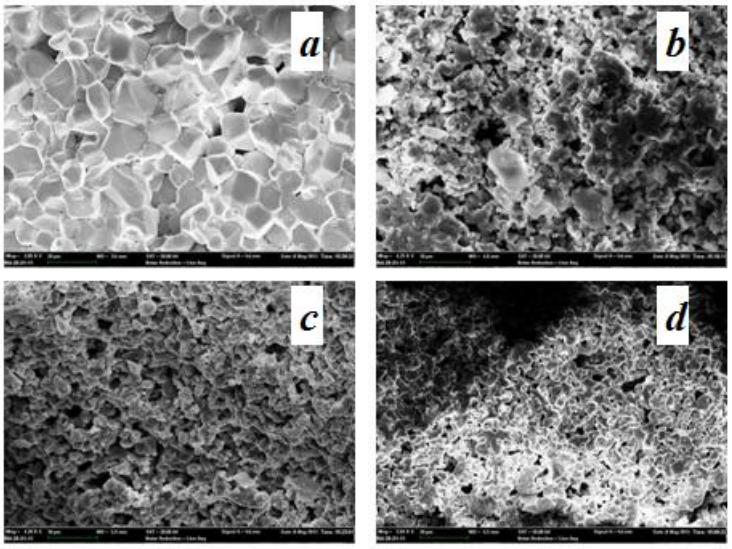

Figure5(*a–d*). *Microstructures $LaMnO_3$ (a – solid state synthesis; b – sorption method; c – coprecipitation method; d – sol-gel method) at room temperature*

In the figures 5 (*a-d*) show SEM-patterns of $LaMnO_3$ microstructures after cooling to room temperature. In the table 3 there are presented structural parameters of all the $LaMnO_3$ samples at room temperature after annealing. Since phase transitions from cubic phases occur in the samples during the process of their cooling to room temperature, the low-temperature phase in case of solid state synthesis is *Pnma* orthorhombic the symmetry. As result $LaMnO_3$ synthesis by wet methods such low-temperature phases are characterized $R\bar{3}c$ rhombohedral symmetry.

Table3. *Structural parameters of $LaMnO_3$ at room temperature, synthesized from different precursors*

Methods of preparation / Structural parameters	Solid state synthesis	Sorption	Co-precipitation	Sol-gel
Space group	*Pnma*	$R\bar{3}c$	$R\bar{3}c$	$R\bar{3}c$
a, Å	5.479(5)	5.507(5)	5.505(5)	5.507(5)
b, Å	7.763(5)	–	–	–
c, Å	5.523(5)	13.525(1)	13.338(1)	13.521(1)
$a_p=c_p$, Å	3.890(5)	–	–	–
b_p, Å	3.882(5)	–	–	–
β, deg	90.45(2)	–	–	–
a_R, Å	–	3.898(5)	3.879(5)	3.897(5)
α, deg	–	89.90(5)	89.59(5)	89.91(5)
V_p, Å^3	58.73(2)	59.21(2)	58.34(2)	59.17(2)
<*D*>, Å	1000	600	1200	600
R_p	0.051	0.037	0.046	0.041

It is previously established [24] that $LaMnO_3$ samples annealing in the oxidic atmosphere leads to the $R\bar{3}c$ phase formation, and that annealing in the air or in the nitric atmosphere leads to *Pnma* phase formation. Our experiments on solid state synthesis lead to formation of nonstoichiometric $LaMnO_{3-\delta}$. Synthesis by wet methods leads to stoichiometric $LaMnO_3$. Let's note that nonstoichiometric $La_{1-x}MnO_3$ (or $La_{1-x}Mn_{1-y}O_3$) is sometimes described by the formula $LaMnO_{3+\delta}$, which appears to be incorrect, as perovskite unit cell can't contain more than three ions of oxygen.

4. CONCLUSION

Because $LaMnO_3$ is a basis of a large number of new multifunctional materials, peculiarities of preparation conditions strongly influence on their structure and physical properties. It was shown that use of various precursors for $LaMnO_3$ formation leads to variations of $LaMnO_3$ structural parameters in processes of synthesis correspond to stoichiometric and nonstoichiometric structures formation. The research results can be used to develop new materials based on $LaMnO_3$ ferroics, in which the properties of nanocrystalline surfaces are the main (in nanodots, nanowires, nanotubes). The obtained results can be used for creation of various solid solutions on the $LaMnO_3$ basis, which can be of a great interest for practical application of multiferroic materials. We are currently completing the studies of the processes of synthesis and physical properties of solid solutions $LaMnO_3 – ABO_3$ (*A* – Ca, Cd, Bi, Y; *B* – Mn, Fe).

ACKNOWLEDGEMENTS

This work was supported by the Russian Ministry of Education and Science (Contract № 3.1246.2014/K). We thank Dr. VB Shirokov, Dr. LE Pustovaya, Dr MP Vlasenko and Dr. BS Koulbuzhev for assistance in the experiments.

REFERENCES

[1] Ahmad T., Lone I.H., Ubaidullah M., Coolhan K., Low-temperature synthesis, structural and magnetic properties of self-dopant $LaMnO_{3+\delta}$ nanoparticles from a metal-organic polymeric precursor, Mater. Res. Bull. 48, 4723 (2013).

[2] Krishnamoorthy C., Sethupathi K., Sankaranarayanan V., Nirmala R., Malik S.K., Magnetic and magnetotransport properties of Ce doped nanocrystalline $LaMnO_3$, J. Alloy Compd. 438, 1 (2007).

[3] Mahmood A., Warsi M.F., Ashiq M.N., Sher M., Improvements in electrical and dielectric properties of substituted multiferroic $LaMnO_3$ based nanostructures synthesized by co-precipitation method, Mater. Res. Bull. 47, 4197 (2012).

[4] Kulandaivelu P., Sakthipandi K., Kumar P.S., Rajendran V., Mechanical properties of bulk and nanostructured $La_{0.61}Sr_{0.39}MnO_3$ perovskite manganite materials, J. Phys. Chem. Solids. 74, 205 (2013).

[5] Tanasescu S., Marinescu C., Maxim F., Raita O., Grecu M-N., Giurgiu L., Thermodynamic properties and spin dynamics of some micro and nanostructured magnetoresistive lanthanum manganites, J. Eur. Ceram. Soc. 26, 3005 (2006).

[6] Mahato N., Banerjee A., Gupta A., Omar S., Balani K., Progress in material selection for solid oxide fuel cell technology: A Review, Prog. Mater. Sci., doi:10.1016/j.pmatsci.2015.01.001 (2015).

[7] Lahmar A., Es-Souni M., Sequence of structural transitions in $BiFeO_3$–$RMnO_3$ thin films (*R*=Rare earth), Ceram. Int. 41, 5721 (2015).

[8] Cao Y., Lin B., Sun Y., Yang H., Zhang X., Synthesis, structure and electrochemical properties of lanthanum manganese nanofibers doped with Sr and Cu, J. Alloy Compd. doi:10.1016/j.jallcom.2015.03.054 (2015).

[9] Aezami A., Abolhassani M., Elahi M., Exchange interaction, electronic structure and magnetic properties of $(LaMnO_3)_m/(SrTiO_3)_n$ superlattices: Ab initio study, J. Alloy Compd. 587, 778 (2014).

[10] Sukhorukov Yu.P., Telegin A.V., Nosov A.P., Gan'shina E.A., Stepantsov E.A., Lombardi F., Winkler D., Magnetorefractive and Kerr effects in the $[La_{0.67}Ca_{0.33}MnO_3/La_{0.67}Sr_{0.33}MnO_3]_n$ superlattices, Superlattice Microst. 75, 680 (2014).

[11] Vila-Fungueirino J.M., Rivas-Murias B., Rodríguez-Gonzalez B., Txoperena O., Ciudad D., Hueso L.E., Lazzari M., Rivadulla F., Room-temperature ferromagnetism in thin films of $LaMnO_3$ deposited by a chemical method over large areas, ACS Appl. Mater. Inter. 7, 5410 (2015).

[12] Goodenough J.B., Longo J.M., Crystallographic and magnetic properties of perovskite and perovskite–related compounds, In: Numerical Data and Functional Relationships in Science and Technology. New Series. Springer-Verlag, Berlin. Heidelberg. New York 1970.

[13] Mochizuki M., Furukawa N., Microscopic model and phase diagrams of the multiferroic perovskite manganites, Phys. Rev. B. 80, 134416 (2009).

[14] Dagotto E. (eds) Nanoscale phase separation and colossal magnetoresistance. The physics of manganites and related compounds. Springer-Verlag, Berlin 2002.

[15] Helmolt R., Wecker J., Holzapfel B., Schultz L., Samwer K., Giant Negative Magnetoresistance in Perovskitelike $La_{2/3}Ba_{1/3}MnO_x$ Ferromagnetic Films, Phys. Rev. Lett. 71, 2331 (1993).

[16] Dagotto E., Hotta T., Moreo A., Colossal magnetoresistant materials: the key role of phase separation, Phys. Rep. 344, 1 (2001).

[17] Varshney D., Dodiya N., Electrical resistivity of alkali metal doped manganites $La_xA_yMn_wO_3$ (*A* = Na, K, Rb): Role of electron-phonon, electron-electron and electron-magnon interactions, Curr. Appl. Phys. 13(7), 1188 (2013).

[18] Varshney D., Choudhary D., Khan E., Electrical transport in the ferromagnetic state of silver substituted manganites $La_{1-x}Ag_xMnO_3$ (x = 0.05 and 0.1), J. Mater. Res. 30(5), 654- (2015).

[19] Troyanchuk I.O., Bushinsky M.V., Sikolenko V., Efimov V., Volkov N.V., Tobbens D.M., Ritter C., Raveau B., Ferromagnetism in single-valent manganites, J. Alloy Compd. 619, 719 (2015).

[20] Cortés-Gil R., Alonso J.M., Rojo J.M., Hernando A., Vallet-Regí M., Ruiz-González M.L., González-Calbet J.M., Hole and electron attractor model: An explanation of clustered states in manganites, Prog. Solid State Ch. 38, 38 (2010).

[21] Laukhin V., Fontcuberta J., Garcıa-Munoz J.L., Obradors X., Pressure effects on the metal-insulator transition in magnetoresistive manganese perovskites, Phys. Rev. B. 56(16), R10009 (1997).

[22] Huang Q., Santoro A., Lynn J.W., Erwin R.W., Borchers J.A., Peng J.L., Greene R.L., Structure and magnetic order in undoped lanthanum manganite, Phys. Rev. B. 55, 14987 (1997).

[23] Zhang Q., Saito F., Mechanochemical synthesis of $LaMnO_3$ from La_2O_3 and Mn_2O_3 powders, J. Alloy Compd. 297, 99 (2000).

[24] Mitchell J.F., Argyrou D.N., Potter C.D., Hinks D.G., Jorgensen J.D., Bader S.D., Structural phase diagram of $La_{1-x}Sr_xMnO_{3+\delta}$: Relationship to magnetic and transport properties, Phys. Rev. B. 54, 6172 (1996).

[25] Gao P., Li N., Wang A., Wang X., Zhang T., Perovskite $LaMnO_3$ hollow nanospheres: The synthesis and the application in catalytic wet air oxidation of phenol, Mater. Lett. 92, 173 (2013).

[26] Proffen Th., Di Francesco R.G., Billinge S.J.L., Brosha E.L., Kwei G.H., Measurement of the local Jahn-Teller distortion in $LaMnO_{3.006}$, Phys. Rev. B. 60, 9973 (1999).

[27] Regaieg Y., Delaizir G., Herbst F., Sicard L., Monnier J., Montero D., Villeroy B., Ammar-Merah S., Cheikhrouhou A., Godart C., Koubaa M., Rapid solid state synthesis by spark plasma sintering and magnetic properties of $LaMnO_3$ perovskite manganite, Mater. Lett. 80, 195 (2012).

[28] Sato K., Chaichanawong J., Abe H., Naito M., Mechanochemical synthesis of $LaMnO_{3+\delta}$ fine powder assisted with water vapor, Mater. Lett. 60, 1399 (2006).

[29] Ohara S., Abe H., Sato K., Kondo A., Naito M., Effect of water content in powder mixture on mechanochemical reaction of $LaMnO_3$ fine powder, J. Eur. Ceram. Soc. 28, 1815 (2008).

[30] Daundkar A., Kale S.N., Gokhale S.P., Ravi V., A low temperature route to prepare $LaMnO_3$. Mater. Lett. 60, 1213 (2006).

[31] Giannakas A.E., Ladavos A.K., Pomonis P.J., Preparation, characterization and investigation of catalytic activity for NO + CO reaction of $LaMnO_3$ and $LaFeO_3$ perovskites prepared via microemulsion method, Appl. Catal. B-Environ. 49, 147 (2004).

[32] Sui Zh-J., Vradman L., Reizner I., Landau M.V., Herskowitz M., Effect of preparation method and particle size on $LaMnO_3$ performance in butane oxidation, Cat. Comm. 12, 1437 (2011).

[33] Bernard C., Durand B., Verelst M., Lecante P., Hydrothermal synthesis of $LaMnO_{3+\delta}$: F.T.I.R. and W.A.X.S. investigations of the evolution from amorphous to crystallized powder, J. Mater. Sci. 39, 2821 (2004).

[34] Dittmar A., Schneider M., Radnik J., Kondratenko E., Herein D., Plasma chemical preparation and characterization of perovskite-type mixed oxides, Prog. Solid. State Ch. 35, 249 (2007).

[35] Najjar H., Lamonier J-F., Mentré O., Giraudon J-M., Batis H., Optimization of the combustion synthesis towards efficient $LaMnO_{3+y}$ catalysts in methane oxidation, Appl. Catal. B-Environ. 106, 149 (2011).

[36] Kakihana M., Arima M., Yoshimura M., Ikeda N., Sugitani Y., Synthesis of high surface area $LaMnO_{3+d}$ by a polymerized complex method, J. Alloys Compd. 283, 102 (1999).

[37] Miyoshi S., Hong J., Yashiro K., Kaimai A., Nigara Y., Kawamura K., Kawada T., Mizusaki J., Lattice creation and annihilation of $LaMnO_{3+\delta}$ caused by nonstoichiometry change, Solid State Ionics. 154-155, 257 (2002).

[38] Moreno L.C., Valencia J.S., Landı´nez Te´llez D.A., Arbey Rodrı´guez J.M., Martı´nez M.L., Roa-Rojas J., Fajardo F., Preparation and structural study of $LaMnO_3$ magnetic material, J. Magn. Magn. Mater. 320, e19 (2008).

[39] Cimino S., Lisi L., De Rossi S., Faticanti M., Porta P., Methane combustion and CO oxidation on $LaAl_{1-x}Mn_xO_3$ perovskite-type oxide solid solutions, Appl. Catal. B-Environ. 43, 397 (2003).

[40] Kraus W., Nolze G., Powder Cell – a Program for the Representation and Manipulation of Crystal Structures and Calculation of the Resulting X-ray Powder Patterns, J. Appl. Cryst. 29, 301 (1996).

[41] Cheng J., Navrotsky A., Zhou X-D., Anderson H.U., Enthalpies of formation of $LaMO_3$ perovskites (M = Cr, Fe, Co, and Ni), J. Mater. Res. 20(1), 191 (2005).

[42] Navrotsky A., Lee W., Mielewczyk-Gryn A., Ushakov S.V., Anderko A., Wu H., Riman R.E., Thermodynamics of solid phases containing rare earth oxides, J. Chem. Thermodynamics. 88, 126 (2015).

[43] Jacob K.T., Attaluri M., Refinement of thermodynamic data for $LaMnO_3$, J. Mater. Chem.13, 934 (2003).

AUTHORS' BIOGRAPHY

Dr Rudskaya Anzhela Grigorievna, is currently an Associate Professor of the Department of Physics, Southern Federal University. She obtained PhD in Solid State Physics "Features of high-temperature phase transitions of Mn-containing perovskites $A'_{1-x}A''_xMnO_3$ (A' – La, Pr; A'' – Ca, Cd, Bi)". The main directions of scientific work: multiferroic synthesis, structure and phase transitions of Mn-containing perovskites, X-ray analysis of functional materials. The author of 70 scientific works, including the chapters of the monographs and books.

Dr Kofanova Natal'aya Borisovna, is currently an Associate Professor of the Department of Physics, Southern Federal University. She obtained PhD in Solid State Physics "The phenomena of the order-disorder in ferroelectric solid solutions with the perovskites structure". The main directions of scientific research: the creation of new functional materials, structures, and the study of phase transitions perovskites and related materials, X-ray analysis. She has published research papers in national and international journals.

Prof. Kupriyanov Michael Fedotovich, is a Professor of Nanotechnological Department, Department of Physics, Southern Federal University. His research interests include the study of the structure and phase transitions in complex oxides, structures of ferroelectric crystals and ceramics, multiferroic, and X-ray analysis of functional materials. The author of over 250 scientific publications, including five published monographs and tree books. He prepared 16 candidates of sciences. He is still actively engaged in teaching and research work.